Pergamon

PII: S0306-4522(99)00587-4

www.elsevier.com/locate/neuroscience

*Neuroscience* Vol. 96, No. 4, pp. 707–722, 2000
IBRO
Published by Elsevier Science Ltd
Printed in Great Britain

# SOMATOMOTOR NEURON-SPECIFIC EXPRESSION OF THE HUMAN CHOLINERGIC GENE LOCUS IN TRANSGENIC MICE*

B. SCHÜTZ,† L. CHEN,† M. K.-H. SCHÄFER,‡ E. WEIHE‡ and L. E. EIDEN†§

†Section on Molecular Neuroscience, Laboratory of Cellular and Molecular Regulation, National Institute of Mental Health, National Institutes of Health, Bethesda, MD 20892, U.S.A.

‡Department of Molecular Neuroimmunology, Institute of Anatomy and Cell Biology, Philipps University, D-35033 Marburg, Germany

**Abstract**—We examined the expression pattern of the vesicular acetylcholine transporter in the mouse nervous system, using rodent-specific riboprobes and antibodies, prior to comparing it with the distribution of vesicular acetylcholine transporter expressed from a human transgene in the mouse, using riboprobes and antibodies specific for human. Endogenous vesicular acetylcholine transporter expression was high in spinal and brainstem somatomotor neurons, vagal visceromotor neurons, and postganglionic parasympathetic neurons, moderate in basal forebrain and brainstem projection neurons and striatal interneurons, and low in intestinal intrinsic neurons. Vesicular acetylcholine transporter expression in intrinsic cortical neurons was restricted to the entorhinal cortex. The sequence of the mouse cholinergic gene locus to 5.1 kb upstream of the start of transcription of the vesicular acetylcholine transporter gene was determined and compared with the corresponding region of the human gene. *Cis*-regulatory domains implicated previously in human or rat cholinergic gene regulation are highly conserved in mouse, indicating their probable relevance to the regulation of the mammalian cholinergic gene locus *in vivo*. Mouse lines were established containing a human transgene that included the vesicular acetylcholine transporter gene and sequences spanning 5 kb upstream and 1.8 kb downstream of the vesicular acetylcholine transporter open reading frame. In this transgene, the intact human vesicular acetylcholine transporter was able to act as its own reporter. This allowed elements within the vesicular acetylcholine transporter open reading frame itself, shown previously to affect transcription *in vitro*, to be assessed *in vivo* with antibodies and riboprobes that reliably distinguished between human and mouse vesicular acetylcholine transporters and their messenger RNAs. Expression of the human vesicular acetylcholine transporter was restricted to mouse cholinergic somatomotor neurons in the spinal cord and brainstem, but absent from other central and peripheral cholinergic neurons.

The mouse appears to be an appropriate model for the study of the genetic regulation of the cholinergic gene locus, and the physiology and neurochemistry of the mammalian cholinergic nervous system, although differences exist in the distribution of cortical cholinergic neurons between the mouse and other mammals. The somatomotor neuron-specific expression pattern of the transgenic human vesicular acetylcholine transporter suggests a mosaic model for cholinergic gene locus regulation in separate subdivisions of the mammalian cholinergic nervous system. © 2000 IBRO. Published by Elsevier Science Ltd.

*Key words:* acetylcholine, cholinergic gene locus, choline acetyltransferase, motorneuron, vesicular acetylcholine transporter.

The cholinergic gene locus (CGL) consists of the genes encoding the vesicular acetylcholine transporter (VAChT) and the acetylcholine biosynthetic enzyme choline acetyltransferase (ChAT).[8] The operon-like character of this gene locus is well-conserved from *C. elegans* to human,[1,9,18] but its transcriptional regulation is more complex in higher animals. The *C. elegans* CGL generates VAChT and ChAT mRNAs via differential splicing from a single primary transcript yielding separate mRNAs with the same first exon.[1] In the rat CNS, transcripts containing this common first exon (called R) are much less abundant than either VAChT or ChAT transcripts, suggesting that most mammalian VAChT and ChAT mRNAs arise from separate transcriptional start sites in the CGL, rather than from the "R" exon common transcriptional start site.[13,17,25,45] In addition, a full-length rat VAChT cDNA whose 5′ end does not contain the R exon has been identified and is abundantly expressed in the rat CNS.[4,6,9] There is also evidence for separate *cis*-regulatory sites within the CGL: transgenes containing regulatory sequences only upstream of the R-exon, and transgenes containing regulatory sequences only downstream of the R-exon, were both able to direct expression of a reporter gene to cholinergic-rich regions of the CNS.[21,26] Studies using transient expression in cultured cells, and with a mouse CGL transgene *in vivo*, indicate that the VAChT gene itself contains *cis*-regulatory sequences for ChAT gene expression.[15,20]

Here, we have compared the pattern of VAChT expression in the mouse central and peripheral nervous system with that reported previously for other mammalian species, including primates.[12,30,34–36,48] We have used this information to directly compare VAChT expression from a transgenic human cholinergic gene locus fragment to endogenous mouse VAChT (mVAChT) expression at the mRNA and protein levels. This approach circumvents the problems inherent in studying promoter activity of a gene potentially containing *cis*-regulatory sequences within its own open reading frame.

## EXPERIMENTAL PROCEDURES

### *Cloning of the mouse cholinergic gene locus*

An approximately 50-kb fragment of the mouse genome was cloned from a bacterial artificial chromosome ES mouse library (Genome

*The sequence reported in this paper has been deposited in GenBank under Accession number AF175307.

§To whom correspondence should be addressed at: Building 36, Room 2A-11, 9000 Rockville Pike, Bethesda, MD 20892, U.S.A.

*E-mail address:* eiden@codon.nih.gov (L. E. Eiden).

*Abbreviations:* CGL, cholinergic gene locus; ChAT, choline acetyltransferase; EDTA, ethylenediaminetetra-acetate; GAPDH, glyceraldehyde-3-phosphate dehydrogenase (EC 1.2.1.12); hVAChT, human vesicular acetylcholine transporter; ISHH, *in situ* hybridization histochemistry; mVAChT, mouse vesicular acetylcholine transporter; NGF, nerve growth factor; NRSE, neuronally restrictive silencer element; PBS, phosphate-buffered saline; PCR, polymerase chain reaction; RT, reverse transcriptase; SSC, standard saline citrate; VAChT, vesicular acetylcholine transporter.

Systems, St Louis, MO, U.S.A.) by polymerase chain reaction (PCR) screening using primers from the VAChT open reading frame conserved between human and rat sequences.[9,13] Two *Hin*dIII fragments from the bacterial artificial chromosome clone, approximately 4 and 7 kb in size, were subcloned into pZErO-2 (Invitrogen, Carlsbad, CA, U.S.A.). Partial sequencing and restriction analysis of the 7-kb fragment showed that it is consistent with the mouse clone obtained by Naciff *et al.*,[27] except for an additional ~700 bp at the 5′ end. The previously uncharacterized 5′-flanking 4-kb *Hin*dIII fragment upstream of the putative "R" exon in the mouse genome and the additional 0.7 kb of the 7-kb *Hin*dIII fragment were sequenced by the dideoxy method of Sanger *et al.*,[33] using the ALFexpress AutoRead 200 Sequencing Kit and the ALFexpress II DNA Analysis System (Amersham Pharmacia Biotech, Piscataway, NJ, U.S.A.). The new sequence has been deposited in Genbank under accession number AF175307. Mouse and human CGL sequences were compared using the "align" feature in GeneWorks 2.5 (Cambridge, MA, U.S.A.). Putative transcription factor binding sites were identified using TFSEARCH (http://pdap1.trc.rwcp.or.jp/research/db/TFSEARCH.html).

### *Construction of a human vesicular acetylcholine transporter transgene, microinjection into fertilized eggs and establishment of transgenic mouse lines*

An 8712-bp genomic fragment from the human CGL in pGEM-7 (Promega, Madison, WI, U.S.A.), extending from ~4 kb upstream of the "R" exon to the middle of the "M" exon,[13] thereby including the VAChT open reading frame, was cut out by *Hin*dIII/*Xba*I digestion and separated from the plasmid DNA by a 10–40% (w/v) sucrose gradient. Fractions containing only the 8.7-kb fragment were pooled, concentrated and the sucrose removed. After ethanol precipitation, the fragment was resuspended in 10 mM Tris–HCl (pH 7.4), 0.1 mM EDTA.

The construct was injected into the male pronuclei of fertilized eggs of FVB mice and the eggs transplanted into pseudopregnant females, who served as foster mothers. To identify transgene-containing siblings in the offspring, DNA from tail snips was obtained by standard salt precipitation methods. Founder mice were identified by PCR amplification of a 129-bp fragment located in the 3′ non-coding region of human VAChT (hVAChT; Table 1, no. 4). To test for the full integration and integrity of the transgene, sequences close to the 5′ end (Table 1, no. 1), the 3′ end (Table 1, no. 2) and the putative VAChT transcription start site (Table 1, no. 3) were amplified by PCR. As an internal control for the integrity of the genomic DNA, a 169-bp fragment from the housekeeping gene glyceraldehyde-3-phosphate dehydrogenase (GAPDH) was amplified. PCR was performed at 94°C for 1 min, 60°C for 45 s and 72°C for 1 min for 32 cycles in a DNA Thermal Cycler (Perkin–Elmer Cetus, Norwalk, CT, U.S.A.). PCR products were separated in 1.5% agarose gels and visualized by ethidium bromide staining.

Three heterozygous founders were each mated to FVB mice, the resulting offspring genotyped, and three transgenic lines established by mating heterozygous siblings.

### *Southern blot analysis*

Analysis of genomic DNA from transgenic and control mice was performed using standard protocols.[32] Briefly, about 10 μg of DNA was digested with *Afl*II/*Xba*I, separated in 0.8% agarose gels and blotted onto nylon membranes. The blots were hybridized with $^{32}$P-labeled probes, generated from the respective PCR amplicons with the Prime-a-gene labeling system (Promega, Madison, WI, U.S.A.). Hybridization was carried out in 6× standard saline citrate (SSC), 0.5% sodium dodecyl sulfate and 100 μg/μl salmon sperm dideoxyribonucleic acid at 42°C overnight. Membranes were washed in 0.2× SSC, 0.5% sodium dodecyl sulfate at 58°C for 2 h and exposed to X-ray film for 4–24 h. The predicted size for the mouse CGL fragment is ~4100 bp, that for the human transgene is ~7600 bp.

### *Reverse transcriptase–polymerase chain reaction analysis of human vesicular acetylcholine transporter expression in mouse*

For reverse transcriptase (RT)–PCR analysis, total RNA was obtained from 50 mg of tissue from regions of mouse brain and peripheral organs using the RNAqueous system (Ambion, Austin, TX, U.S.A.) following the manufacturer's instructions. About 2 μg of total RNA was digested with 1 μg/μl DNase I for 1 h at 37°C to eliminate contaminating DNA and then divided into two equal fractions. The DNase I step was of particular importance, because the mammalian VAChT gene has no introns. One fraction was subject to reverse transcription using the SuperScript system (GibcoBRL Life Technology, Gaithersburg, MD, U.S.A.), the other fraction served as a non-RT control for DNA contamination. In addition to the above-described hVAChT and GAPDH amplicons, a 109-bp fragment from mVAChT was amplified (Table 1). PCR conditions were essentially as described above. Control PCR for primer pair cross-reactivity using mVAChT primers and an hVAChT cDNA template and vice versa did not result in amplification of PCR products. Following PCR, the amplified DNA was separated on 1.5% agarose gels and subjected to Southern blot analysis (see above).

### *Tissue preparation for histological analysis*

All animal procedures were performed according to National Institutes of Health (Bethesda, MD, U.S.A.) guidelines for the care and use of laboratory animals under an animal protocol approved by the NIMH-IRP Animal Care and Use Committee. All efforts were made to minimize animal suffering and to reduce the number of animals used.

From each of the three transgenic mouse lines, six transgene-containing animals (breeding generations F2 and F3) and four non-transgenic siblings were processed for histological analysis. The mice were killed by $CO_2$ inhalation and the tissue to be examined prepared in the following ways. (1) For immunohistochemical analysis, the mice were perfused transcardially with cold phosphate-buffered saline (PBS) to clear the organs of blood, followed by Bouin Hollande fixative, containing 4% (w/v) picric acid, 2.5% cupric acetate, 3.7% formaldehyde and 1% glacial acetic acid. Following perfusion, the

Table 1. Polymerase chain reaction primer sequences and amplicon sizes used for studying the human vesicular acetylcholine transporter transgene in the mouse

| Primer pair | Sequence | Amplicon size (bp) |
|---|---|---|
| 1 | 5′-AGCCTGCCTCTTGCCGCAGTCCTTAAGCA-3′ | 479 |
| | 5′-TTCCCAGTCACCGCACTTCCCCAACCC-3′ | |
| 2 | 5′-CAGGGGTGGATTGTCAGGGTCTGGAGGCAA-3′ | 328 |
| | 5′-TCAAAGGAACAAAGTGGCCCCAGTCAGCC-3′ | |
| 3 | 5′-AAGGGGCCTCGAGGAACCGGCTGCCG-3′ | 318 |
| | 5′-CGAGTCCCAGCCCCCGAGTGGTGCCCGGGCCA-3′ | |
| 4 | 5′-CCCGTTCCATATCCCTTTCTCTCTTGTCCAA-3′ | 129 |
| | 5′-CACAGGGGAGCCGCAGGTGGGGACTCAGGGTC-3′ | |
| GAPDH | 5′-CGACCCCTTCATTGACCTCAACTACATG-3′ | 169 |
| | 5′-CGGCCTCACCCCATTTGATGTTAGTGGG-3′ | |
| mVAChT | 5′-CAGTCTAACCCCCTCTCCAAACACACTCG-3′ | 109 |
| | 5′-CAGTAGGTGGTTGGTGATCACCGGTACAC-3′ | |

1, 2, 3 and 4 are hVAChT-specific primer sets. For each primer pair, the first sequence is the forward, the second sequence the reverse primer.

brains, spinal cords and several peripheral organs were removed and immersion-postfixed overnight. Following extensive washes in 70% 2-propanol, the tissues were dehydrated, cleared with xylene and embedded in paraffin. Sections were cut at 7 μm with a microtome and processed for antibody staining (see below). (2) For the localization of hVAChT and mVAChT transcripts in tissue sections by *in situ* hybridization histochemistry (ISHH), brains, spinal cords and peripheral organs were immediately frozen in isopentane at −50°C and stored at −70°C. Sections were cut at 20 μm in a cryostat, mounted on silanized glass slides, dried for 5–10 min at 38°C on a warm plate and stored at −70°C until use.

*Characteristics of specific antisera against the mouse and human vesicular acetylcholine transporter*

For the detection of endogenous mVAChT, the rabbit antiserum no. 80259 raised against the C-terminal peptide CEDDYNYYSRS of rat VAChT was used.[48] This antiserum cross-reacts with mVAChT, but not with hVAChT (note: the mouse sequence is identical to rat in this region). For the detection of the transgenic hVAChT in mouse tissue, the rabbit antiserum no. 80153 raised against the C-terminal peptide CEDDYNYYYTRS of hVAChT was used.[36] This antiserum does not show any cross-reactivity with mVAChT, which was proven by the absence of staining of cholinergic cell bodies and terminals in non-transgenic mouse tissue. Both antisera were employed at final dilutions of 1:1000–1:2000 in immunohistochemistry, as described below.

*Immunohistochemistry*

Immunohistochemistry for mouse and human VAChT was carried out on deparaffinized tissue sections as described, with some modifications.[31,34] Briefly, sections were deparaffinized in xylene, rehydrated through a graded series of 2-propanol, incubated in methanol/$H_2O_2$ to block endogenous peroxidase activity and then incubated in 10 mM sodium citrate buffer (pH 6.0) at 95°C for 10 min in a pressure cooker. After several rinses in 50 mM PBS, sections were incubated in PBS containing 5% bovine serum albumin for 30 min. The primary antibodies were applied in PBS/1% bovine serum albumin and incubated at 16°C overnight followed by 2 h at 37°C. After several washes in distilled water followed by rinsing in PBS, sections were incubated with species-specific biotinylated secondary antibodies (Dianova, Hamburg, Germany) for 45 min at 37°C, washed several times and incubated for 30 min with the avidin–biotin–peroxidase complex reagents (Vectastain Elite ABC kit, Boehringer, Ingelheim, Germany). Immunoreactions were visualized with 3,3′-diaminobenzidine (Sigma, Deisenhofen, Germany) enhanced by the addition of 0.08% ammonium nickel sulfate (Fluka, Buchs, Switzerland), resulting in a dark blue staining. Immunostained sections were analysed and photographed with an AX Olympus microscope.

*Generation of specific complementary RNA probes for the mouse and human vesicular acetylcholine transporters*

Specific riboprobes for mVAChT and hVAChT mRNAs were generated by *in vitro* transcription from a pBluescript II KS+ vector containing a cDNA fragment corresponding to nucleotides 2222–3021 of mVAChT[27] and from a pGEM-7 vector containing a genomic fragment from the human CGL[13] (nucleotides 6951–7682), respectively, using [$^{35}$S]UTP-labeled nucleotides. To increase tissue penetration of probes, the generated transcripts were reduced to about 150-nucleotide fragments by limited alkaline hydrolysis, as described by Angerer *et al.*[2] The possibility of cross-reactivity of the hVAChT riboprobe with mVAChT mRNA was excluded by performing *in situ* hybridization experiments (see below) on sections from non-transgenic mice, but rich in cholinergic cell bodies. Even after four weeks of exposure, no specific signal was detectable.

In situ *hybridization histochemistry*

*In situ* hybridization experiments were performed on 20-μm cryostat sections as described previously, with a few modifications.[39] Briefly, for pretreatment, sections were air dried for 15 min, fixed in freshly prepared 4% (w/v) paraformaldehyde in PBS for 60 min at room temperature and washed for 3×10 min in 10 mM PBS. After a brief wash in distilled water, sections were acetylated with triethanolamine/acetic anhydride for 10 min at room temperature, followed by a 5-min wash in distilled water. The sections were then dehydrated through a graded series of ethanol (50%, 80%, 96%, 100%; each 2 min) and incubated for 2×5 min in chloroform at room temperature. After a 2-min incubation in 100% and 96% ethanol, sections were air dried for 30 min and directly used for hybridization, or stored at −20°C until use.

For hybridization, sections were covered with 30–40 μl of hybridization solution, containing 50% formamide, 0.6 M NaCl, 10 mM Tris (pH 7.4), 1 mM $Na_2EDTA$, 1×Denhardts, 10% dextran sulfate, 100 μg/ml sheared salmon sperm DNA, 0.05% (w/v) *E. coli* MRE600 tRNA, 20 mM dithiothreitol, 50 000 d.p.m./μl riboprobe and coverslipped. Hybridization was carried out overnight at 60°C in a humid chamber. After hybridization, coverslips were removed in 2×SSC at room temperature and the sections washed in the following order: 20 min in 1×SSC, 45 min at 37°C in RNase solution containing 20 μg/ml RNase A and 1 U/ml RNase T1, 20 min in 1×SSC, 20 min in 0.5×SSC, 20 min in 0.2×SSC, 60 min in 0.2×SSC at 60°C, 10 min in 0.2×SSC at room temperature and 10 min in distilled water. Finally, sections were dehydrated in 50% and 70% ethanol and air dried at room temperature. For visualization of hybridization signals, sections were first exposed to Amersham β-Max autoradiography film for one to three days to estimate further exposure times, then coated with Kodak NTB2 emulsion, exposed for one to four weeks at 4°C and developed. Sections were counterstained with hematoxylin/eosin and hybridization signals documented on Kodak Ectachrome II color slide films using a Nikon Labophot 2 microscope and the slides digitized with a Polaroid slide scanner.

## RESULTS

### *Expression of the vesicular acetylcholine transporter in the mouse central nervous system*

Mapping the mouse cholinergic nervous system is a prerequisite for defining the roles of *cis*-regulatory elements of the CGL, with transgenes that target cholinergic neurons or subsets of cholinergic neurons. Limited information about the anatomical distribution of cholinergic cells and their projection fields in the mouse central and peripheral nervous systems is available.[19,26,27] Therefore, the distribution of VAChT and VAChT mRNA in the adult mouse CNS was analysed in detail.

An mVAChT-specific cRNA probe was used for *in situ* hybridization of serial coronal brain sections. This cRNA spans the 3′ non-coding region of the VAChT mRNA and shows only minimal cross-reactivity with rat or hVAChT (data not shown). VAChT mRNA is specifically expressed within the well-defined cholinergic nuclei of the brain present in other mammalian species (Fig. 1).[40] VAChT mRNA was present in the basal nuclear complex in projection neurons of the medial septum, in the nuclei of the vertical and horizontal limbs of the diagonal band (Fig. 1A), and in the basal nucleus of Meynert (Fig. 1B), and also in interneurons of the caudate–putamen (Fig. 1B). In the midbrain, the medial habenular nucleus (Fig. 1B) and cell groups in the hypothalamus (data not shown) expressed VAChT mRNA. In the brainstem, all somatomotor and preganglionic parasympathetic nuclei of the cranial nerves (Fig. 1C–G; data shown for motor nuclei of cranial nerves 3, 5, 7, 10 and 12), and the pedunculopontine and lateral dorsal tegmental nuclei (Fig. 1D) were labeled. Finally, the motor neurons in the ventral horn of the spinal cord (Fig. 1H), and the preganglionic sympathetic neurons in the intermediolateral and intermediomedial cell columns (data not shown), strongly expressed VAChT mRNA. VAChT mRNA was not detected in neocortical intrinsic neurons.[34,37]

The VAChT antipeptide antiserum no. 80259, originally developed for the detection of rat VAChT, was used to label the identical C-terminal VAChT epitope in cholinergic

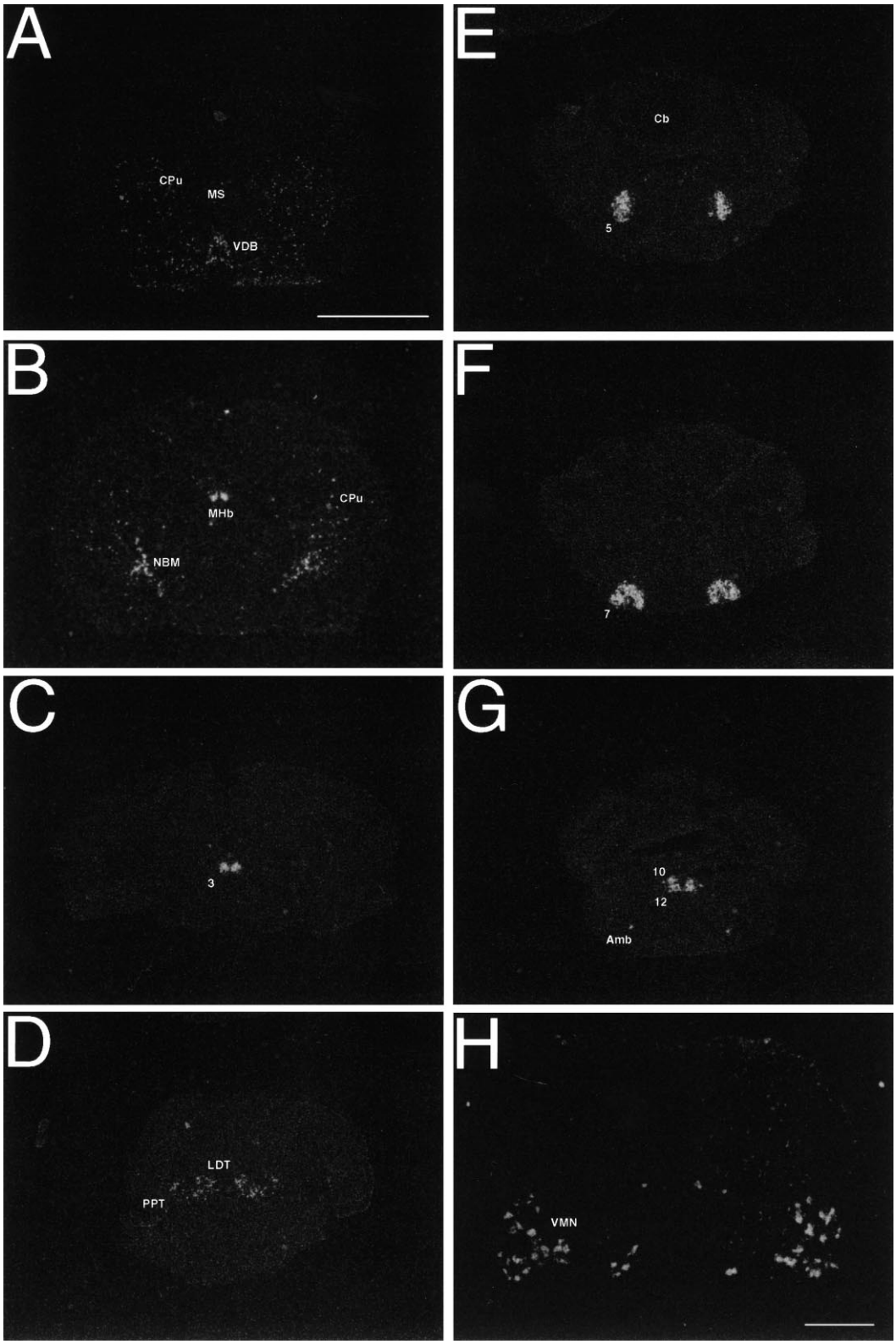


Fig. 1. Distribution of VAChT mRNA-expressing cell groups in the mouse CNS. Dark-field autoradiograms of coronal sections in rostral (A) to caudal (H) orientation show VAChT ISHH signals specifically in well-accepted classical cholinergic cell groups after hybridization with a $^{35}$S-labeled cRNA probe. Exposure times of X-ray films were 24 h. VAChT-expressing nuclei in the basal nuclear complex include the medial septal nucleus (MS), the nucleus of the ventral limb of the diagonal band (VDB) and the basal nucleus of Meynert (NBM). Cholinergic interneurons in the striatum are detected scattered throughout the caudate–putamen (CPu). In the diencephalon, the medial habenular nucleus (MHb) is intensely labeled. In the brainstem, all somatomotor and preganglionic parasympathetic nuclei of the cranial nerves express VAChT mRNA, shown here for the oculomotor nucleus (3), the trigeminal motor nucleus (5), the facial motor nucleus (7), the dorsal motor nucleus of vagus (10), the hypoglossal nucleus (12) and the nucleus ambiguus (Amb). In addition, cell groups in the mesopontine tegmentum, including the pedunculopontine nucleus (PPT) and the laterodorsal tegmental nucleus (LDT), are labeled. In the spinal cord, the motorneurons in the ventral horn (VMN) are heavily covered with VAChT hybridization signals. Cb, cerebellum. Scale bar = 2 mm (A; also applies to B–G), 250 μm (H).

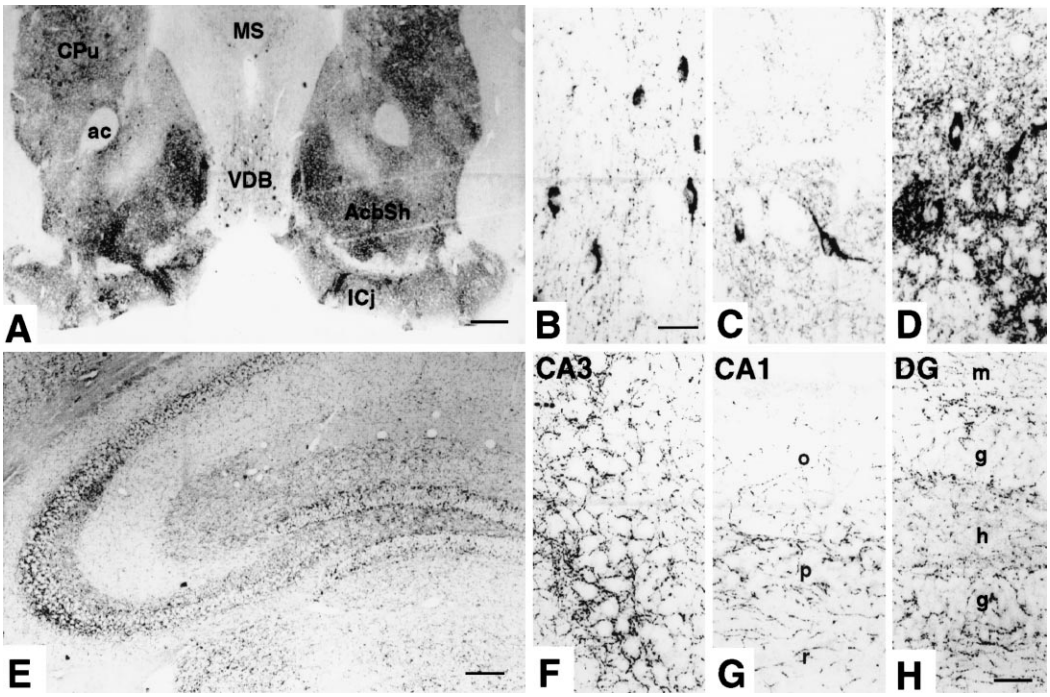


Fig. 2. VAChT-positive cell bodies and terminals in mouse basal forebrain and hippocampus. In a coronal section through the basal nuclear complex (A), VAChT immunoreactivity is present in cell bodies of the medial septal nucleus (MS) and in the nucleus of the vertical limb of the diagonal band of Broca (VDB). The caudate–putamen (CPu), the shell of the nucleus accumbens (AcbSh) and the islands of Calleja (ICj) are all characterized by an intense punctate VAChT fiber staining. The VAChT-immunoreactive cells of the medial septal nucleus in B and the striatal interneurons in C are not extensively targeted by cholinergic fibers. The islands of Calleja contain intrinsic, VAChT-positive neurons, which are supposed to contribute to the patch-like innervation pattern by local ramifications (D). In the rostral hippocampal formation (E), a region-specific density of varicose fibers is visible in the different regions and layers. (F) In the CA3 region, VAChT-positive terminals are most dense in the pyramidal cell layer. (G) VAChT-positive innervation throughout the CA1 region. The density of VAChT innervation is high in the pyramidal cell layer (p) and only moderate in strata oriens (o) and radiatum (r). (H) Different densities of VAChT terminal fibers in the layers of the dentate gyrus (DG). The highest fiber density is present along the borders between the molecular (m) and the granular (g) cell layers, and only moderate within these layers and in the hilus (h). Note the absence of VAChT-positive neuronal cell bodies in all regions of the hippocampus. Scale bars = 250 μm (A), 25 μm (B; also applies to C and D), 100 μm (E), 25 μm (H; also applies to F and G).

cell bodies, synapses and terminal fields of the mouse CNS. VAChT immunoreactivity within the cell groups and terminal fields of the major forebrain cholinergic circuits is shown in Figs 2 and 3. The basal nuclear complex contains the cell bodies for the cholinergic projections systems Ch1–Ch4 and Ch7.[24] These are the Ch1 and Ch2 projections from the medial septal nucleus and the diagonal band of Broca to the hippocampus, the Ch3 projection from the horizontal limb of the diagonal band to the olfactory bulb, the Ch4 projection from the nucleus basalis of Meynert to the cortex and amygdala, and the Ch7 projection from the magnocellular preoptic area to the interpeduncular nucleus. Intense VAChT staining is exemplified in neuronal cell bodies of the medial septal nucleus (Fig. 2A, B), the vertical limb of the diagonal band of Broca (Fig. 2A) and the basal nucleus of Meynert (Fig. 3B).

A high fiber density was observed in the shell of the nucleus accumbens (Fig. 2A), in the islands of Calleja (Fig. 2A, D) and in the striatum (Fig. 2C). VAChT immunoreactivity in nerve terminals of the accumbens and islands of Calleja was notable for dense patches of neuropil surrounded by a matrix that was only moderately VAChT positive. These patches contained VAChT-immunoreactive cell bodies, which contribute by local ramification to this intense terminal staining (Fig. 2D). The origin of extrinsic fibers targeting these nuclei is unclear.

In the hippocampus, cholinergic terminals were found in all cell layers of the CA1 and CA3 regions, and of the dentate gyrus (Fig. 1E). The densest fiber network was detected in the pyramidal cell layer of the CA1 (Fig. 1G) and CA3 (Fig. 1F) regions, and along the borders between the granular and molecular cell layers of the dentate gyrus (Fig. 1H). No VAChT-positive neuronal profiles were detected in mouse hippocampus.

The cerebral cortex receives extrinsic cholinergic innervation from the Ch4 projection (Fig. 3F–H). VAChT-immunoreactive fibers and terminals formed a scattered network throughout all cortical layers, with the density being lowest in the most superficial layer (Fig. 3H). The sparse but panneocortical intrinsic cholinergic system seen in the rat was not observed in mouse cortex. Instead, intrinsic cholinergic neurons, at least as detected by VAChT immunohistochemistry, were confined to the entorhinal cortex, where they formed a small cluster of weakly stained neurons (Fig. 3G).

The amygdala, another major Ch4 projection field, was characterized by intense terminal staining, especially in the basolateral nucleus of the amygdala (Fig. 3A). The density of this fiber staining was comparable to the intense punctate pattern of cholinergic immunoreactivity in striatal interneurons (Fig. 3A, B).

The mouse diencephalon is a source of cholinergic neurons and the target of cholinergic fibers. In the thalamus (Fig. 3A), the small neurons of the medial habenular nucleus, which contribute significantly to the Ch7 projection to the interpeduncular nucleus, stained intensely for VAChT (Fig. 3C). VAChT-positive terminal fields have their origin in brainstem nuclei (see below) and are distributed heterogeneously in the thalamus, being most dense in the lateral habenular nucleus (Fig. 3A). The central medial nucleus, the dorsolateral nuclei and

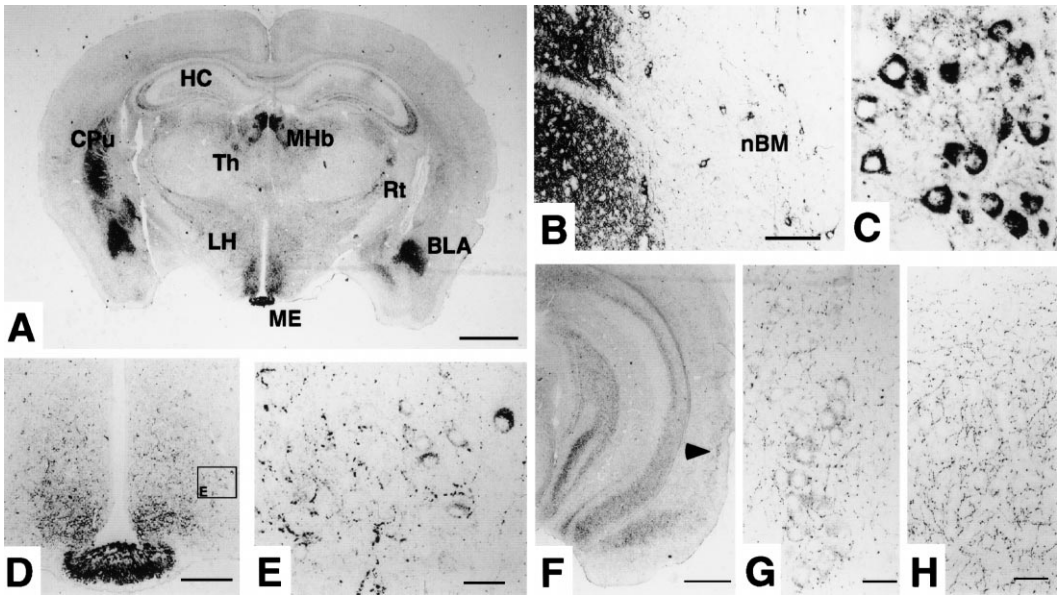


Fig. 3. VAChT immunoreactivity in neuronal cell bodies and terminal fields in the caudal part of the basal nuclear complex, the diencephalon and cortex. (A) Region-specific density of VAChT-immunoreactive cell bodies and terminal fields. In the basal nuclear complex, a strong staining is present in the caudate–putamen (CPu) and in the basolateral amygdala (BLA). In the thalamus (Th), the densely packed neurons of the medial habenular nucleus (MHb) are heavily stained with the VAChT antiserum, which is shown in greater detail in C. In the hypothalamus, the cholinergic terminals in the median eminence (ME) are most prominent. (B) The neurons of the nucleus basalis of Meynert (nBM) are located in a region without a dense cholinergic innervation, compared to the heavy patch-like staining of the nearby caudate–putamen. (D) Higher magnification of the median eminence and the adjacent arcuate nucleus in the hypothalamus. The staining in the arcuate nucleus is due to cholinergic neurons and terminals. (E) Some VAChT-positive cell bodies and intermingling terminals in the lateral hypothalamus. (F) Low magnification of a coronal section through the entorhinal cortex, showing region-specific densities of VAChT-positive innervation. The arrowhead points toward a small group of VAChT-positive neurons, shown at higher magnification in G. These cells are themselves targets of cholinergic fibers, visualized as punctate staining around the cell bodies. (H) A section from the parietal cortex shows that VAChT immunoreactivity in terminals is detectable in all cortical cell layers. Note the absence of intrinsic cholinergic neurons. HC, hippocampus; LH, lateral hypothalamus; Rt, reticular nucleus. Scale bars = 1 mm (A), 100 μm (B), 200 μm (D), 25 μm (E; also applies to C), 500 μm (F), 25 μm (G, H).

the reticular nucleus showed moderate fiber densities, whereas the ventral posterior part of the thalamus was almost devoid of cholinergic fibers. In the hypothalamus, cholinergic neurons could be visualized by VAChT immunoreactivity in the arcuate nucleus (Fig. 3D) and in the ventromedial nucleus (Fig. 3E). Whereas most of the hypothalamic nuclei showed a moderate density of innervating cholinergic fibers (Fig. 3A), the median eminence contained a heavily stained cholinergic terminal field (Fig. 3D), thought to represent a short projection system from the arcuate nucleus.[35]

Cholinergic cell groups that project to the thalamic relay nuclei have been localized to the mesopontine tegmentum and are termed the "ascending reticular activating system", responsible for modulation of sensory input into the thalamus as a function of state of arousal.[41] The Ch5 projection system originates in the pedunculopontine tegmental nucleus (Fig. 4E) and has terminal fields in all thalamic nuclei. The Ch6 projection originates in the laterodorsal tegmental nucleus (Fig. 4E) and projects predominantly to thalamic nuclei associated with limbic functions. Besides receiving fibers from the mesopontine tegmentum, the superior colliculi are the terminal field of the Ch8 projection system, which originates in the parabigeminal nucleus.[47] This ascending projection targeted predominantly the intermediate gray cell layer, whereas the superficial gray cell layer showed only a moderate density of cholinergic terminals (Fig. 4B). The periaqueductal gray (Fig. 4B) and the raphe nuclei (Fig. 4E), pain processing areas in the brainstem, received a significant cholinergic innervation, visualized by VAChT terminal staining. Besides these structures, cholinergic terminals can also be detected in the pineal gland (Fig. 4D).

Cholinergic neurons that lie within the CNS but project to the periphery include several somatoefferent and visceroefferent cell groups residing in the brainstem and spinal cord (Fig. 4C, E, G). These cell groups could be distinguished from ascending projection neurons on the basis of more intense somal staining, as well as the higher density of VAChT-positive homotypic synapses on somatomotor compared to projection neuron cell groups. For example, the neurons of the somatomotoric facial motor nucleus (Fig. 4G) showed intense staining both in the somata and in surrounding puncta with the VAChT antiserum, while the cell bodies of the laterodorsal tegmental nucleus were only poorly contacted by cholinergic fibers (Fig. 4F).

### *Comparison of mouse and human cholinergic gene locus upstream sequences*

The study of a human transgene in a mouse background (see below) is appropriate to the extent that potential gene-regulatory sequences contained in the transgene are conserved between the two species. A total of 5.1 kb of mouse genomic DNA in the 5′-flank of the VAChT open reading frame was sequenced and compared to its human counterpart. The new sequence has an *Mbo*I site at its 3′ boundary, 633 bp upstream of the start of translation of VAChT (+1). This site corresponds to the 5′ end of the mouse genomic sequence published by Naciff *et al.*[27] The 5′ end of the new mouse sequence extends approx. 900 bp further upstream than the known human sequence. A stretch of ~185 bp, corresponding to a portion of the non-coding

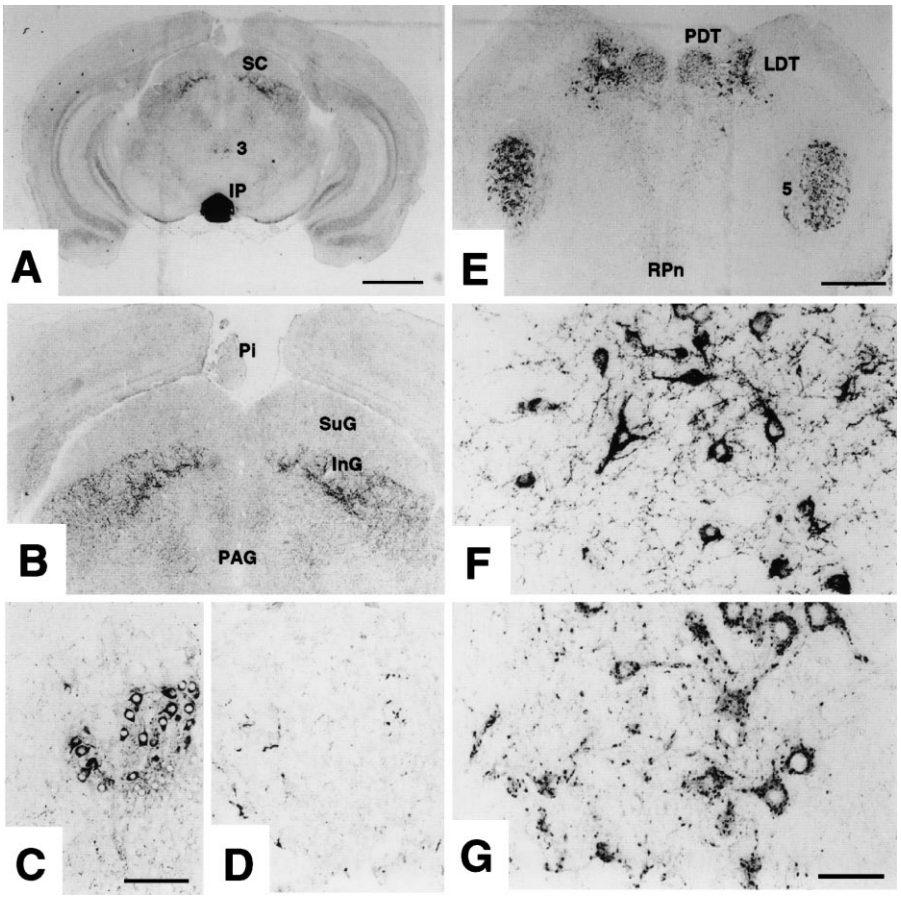


Fig. 4. VAChT immunoreactivity in cell groups and terminals in the brainstem. (A–E) The brainstem is the origin and terminal field of cholinergic projections. All the somatomotor neurons, which project into the periphery, can be visualized by anti-VAChT antibodies, shown here for the oculomotor nucleus (C) and the motor nucleus of the trigeminus (E). Ascending cholinergic projections to the thalamus have their origin in the mesopontine tegmentum, exemplified by VAChT staining in the posterodorsal nucleus (PDT) and laterodorsal tegmental nucleus (LDT). Ascending projection neurons (F) and descending somatoefferent neurons (G) can be discriminated by the number of cholinergic boutons targeting the cell bodies, which is low in the former and high in the latter. The superior colliculi (SC) are the terminal field of the Ch8 projection, originating in the parabigeminal nucleus. These fibers terminate predominantly in the intermediate gray layer (InG) and almost spare the superficial gray layer (SuG). At the level of the superior colliculi, the interpeduncular nucleus (IP) stains heavily for VAChT. Terminals are also detectable in the periaqueductal gray (PAG) and in the pineal gland (Pi), shown at higher magnification in D. 3, Oculomotor nucleus; 5, motor nucleus of trigeminus. Scale bars = 1 mm (A), 100 μm (C), 500 μm (E; also applies to B), 50 μm (G; also applies to D and F).

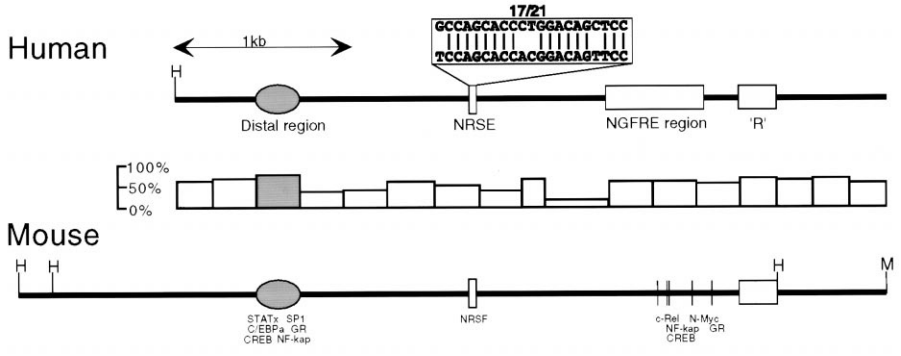


Fig. 5. Comparison of local homology within the mouse and human CGL 5′ flank: conservation of control regions in the mammalian cholinergic gene locus. Sequence identities between corresponding regions in the mouse (GenBank Accession no. AF175307) and the human gene (GenBank Accession no. U10554) are indicated by dark grey (>70% identity), grey (50–70% identity) or white (<50% identity) bars (for each 250-bp segment of DNA) that appear between the schematized mouse and human genes. Regulatory regions are indicated on and named below the human gene, and the positions of putative *trans*-acting factors are indicated by vertical bars on the mouse sequence and the factor named below. A detailed sequence comparison between the mouse and human NRSEs is shown at the top. A, *Alf*II site; H, H*ind*III site; M, M*bo*I site; NGFRE, nerve growth factor-responsive element; "R", R exon.

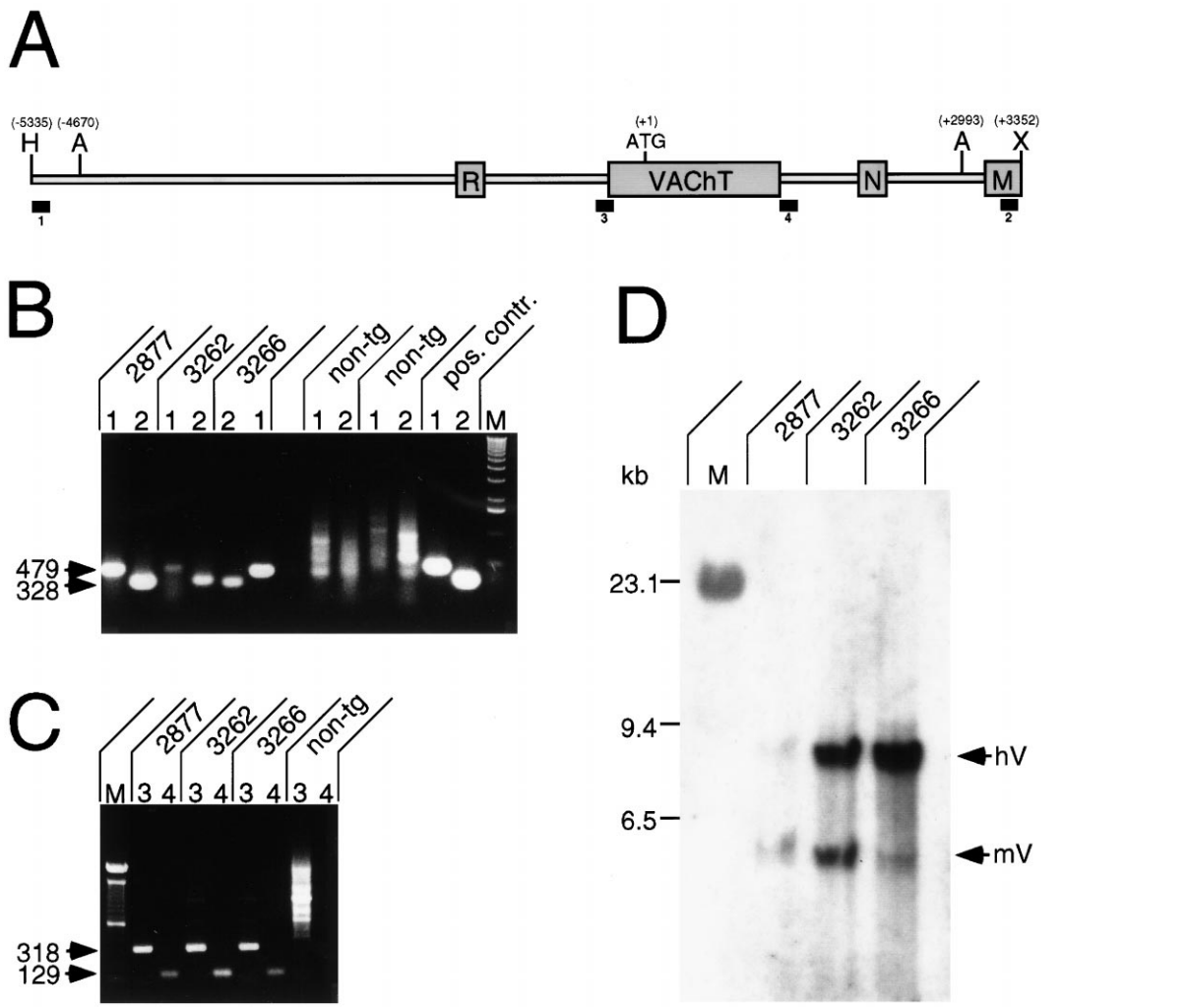


Fig. 6. Schematic representation of the human CGL transgene and its integration into the mouse genome. (A) The human transgene spans from a *Hin*dIII site at −5335 to an *Xba*I site at + 3352, compared to the VAChT translation start site ( + 1). It encompasses the VAChT open reading frame and the three ChAT non-coding exons "R", "N" and "M", together with ~4 kb of gene-regulatory sequence upstream of the "R" exon. The sites of PCR amplification with hVAChT-specific primer pairs (labeled 1–4) are shown below the transgene. The region of the CGL downstream of the "M" exon includes 2.5 kb of intervening sequence and the exon that begins the ChAT open reading frame in both rodent and human. This region is not included in the human CGL transgene. A diagrammatic representation of the cholinergic gene loci of both rat and human can be found in Usdin *et al.*[45] and Eiden.[8] (B) PCR analysis from five mice after transgene injection. Three mice (2877, 3262 and 3266) have a full integration of the human transgene into their genome, visualized by the amplification of a 479-bp fragment from the 5′ end (primer pair 1) and a 328-bp fragment from the 3′ end of the transgene (primer pair 2). Two animals show no hVAChT-specific amplification and are therefore considered to be non-transgenic (non-tg). The positive controls include PCR amplification using 10 pg of subcloned human CGL. (C) PCR analysis of three transgenic and one non-transgenic animals, showing the integrity of the VAChT transcriptional unit. In all three transgenic animals, a 318-bp fragment spanning the VAChT transcription start site and a 129-bp fragment spanning the stop codon are detectable. (D) Southern blot analysis to estimate transgene copy number. Roughly equal amounts of genomic DNA from the three transgenic animals were digested with *Afl*II and *Xba*I, blotted and hybridized with a mouse/hVAChT common probe. The hVAChT band has the expected size of ~7.6 kb; the mVAChT band appears to be ~4.1 kb in size. Comparing human- and mouse-specific signal intensities, the three mouse lines had one to more than four copies of the transgene per genome. A, *Afl*II site; H, *Hin*dIII site; X, *Xba*I site.

ChAT "R" exon in the mouse[25] was identical to the sequence reported here.

The schematic illustration in Fig. 5 shows a comparison of mouse and human homologous domains throughout the VAChT 5′ flanking region. The overall identity between the sequences was 59%, with several domains previously inferred to be important in cholinergic cell-specific transcription[13,21,22] showing higher levels of sequence identity. For example, a potential transcription-enhancing distal region in the human gene was 74% identical to the corresponding mouse region, which was also the highest overall score found in this comparison, using 250-bp segments as units. This region is characterized by the presence of multiple potential transcription factor binding sites, and several are conserved between mouse and human. The mouse neuron restrictive silencer element (NRSE), a target sequence for the neuronally restrictive silencing factor (REST/NRSF),[7,38] which may function to silence the CGL in non-cholinergic cell lines,[13,22,44] was found to be 81% identical to the human NRSE and 100% identical to the rat NRSE. A putative nerve growth factor (NGF)-response element region located directly upstream of the "R" exon in rat and human also showed a high overall sequence identity between mouse and human, consistent with the importance of this region in growth factor-mediated regulation of the CGL.[5,16] The "R" exon, the furthest upstream non-coding exon for the ChAT and VAChT genes, showed a 64% identity with human and an 89% identity with its rat counterpart.

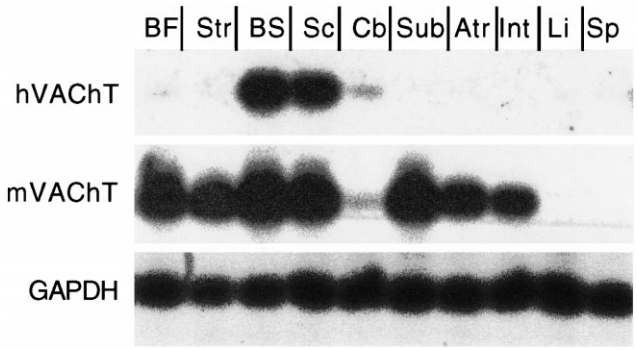


Fig. 7. Expression of mVAChT and transgenic hVAChT in subdivisions of the central and peripheral nervous systems. Shown here are data from line 3262, representative of all three mouse lines. RNA preparations were subjected to RT–PCR analysis, blotted and hybridized with species-specific VAChT probes. Endogenous mVAChT is expressed in the basal forebrain (BF), striatum (Str), brainstem (BS), spinal cord (Sc), submandibular gland (Sub), and in the intestine (Int), atrial region of the heart (Atr), structures known to contain cholinergic neurons. Peripheral organs with no mVAChT signal include the liver (Li) and spleen (Sp). Signals for transgenic hVAChT mRNA expression are restricted to the brainstem and spinal cord. The weak RT–PCR signal in the cerebellum, also seen with mVAChT, may be due to trace contamination of the cerebellum mRNA with genomic DNA due to incomplete DNase digestion. It should be mentioned here that differences in RT–PCR amplicon levels between any two tissues do not reflect differences in VAChT mRNA copy number per cholinergic nucleus or cell body because of the differences in the ratio of cholinergic to non-cholinergic cells in tissue preparations. Amplification of a GAPDH fragment was used to standardize signal intensities.

*Expression of a fragment of the human cholinergic gene locus in the mouse cholinergic nervous system*

To identify regions in the CGL that are important for the cell type-specific expression of VAChT and ChAT *in vivo*, we tested a fragment of the human CGL for its ability to confer correct expression of hVAChT to mouse cholinergic neurons. An ~8.7-kb fragment of the human CGL, encompassing the VAChT open reading frame itself, together with ~5 kb of 5′-flanking and ~1.8 kb of 3′-flanking sequences (Fig. 6A), was chosen. This region of the CGL extends 5′-ward through all known putative regulatory elements of the gene up to the matrix attachment site identified previously in the human gene,[44] and 3′ to the M-exon, considered to be the furthest downstream major transcriptional start point for the ChAT gene.[17,25] This construct was injected into the pronuclei of fertilized mouse eggs and the resulting offspring analysed for transgene integration. Three animals were identified that showed a complete integration of the transgene into the mouse genome by PCR amplification of sequences close to the 5′ and 3′ ends of the transgene (Fig. 6B). The integrity of the VAChT transcriptional unit was shown by PCR amplification of two fragments, one spanning the region of VAChT transcription start and the other one the region of the stop codon (Fig. 6C). Using these three animals as founder mice, three transgenic mouse lines were established which had stable transgene integration and transmitted it to their offspring.

DNA from animals from all three transgenic lines was Southern blotted (Fig. 6D) to estimate transgene copy number. Signal intensities of a ~7.6-kb *Afl*II human CGL fragment and a ~4.1-kb *Afl*II/*Xba*I mouse CGL fragment were compared using a $^{32}$P-labeled DNA probe hybridizing to both mVAChT and hVAChT. All three lines had one to more than four copies of the transgene per genome.

The expression pattern of the human transgene in the mouse central and peripheral nervous system was analysed by RT–PCR, *in situ* hybridization and immunohistochemistry. Figure 7 shows the results from RT–PCR analysis of line 3262, representative of all three lines investigated. Regions of the mouse CNS containing cholinergic cell bodies were compared with peripheral organs containing autonomic cholinergic ganglia/neurons and some organs without intrinsic cholinergic innervation. In comparison to the expression levels of endogenous VAChT assessed by ISHH (see above), mVAChT signals generated by RT–PCR are highest in the brainstem and spinal cord, followed by the basal forebrain, striatum and submandibular gland. Tissues with the weakest signals were the atrium and intestine. Mouse VAChT was not expressed in the liver or spleen, consistent with a lack of cholinergic intrinsic neurons in these organs. Human VAChT mRNA was detectable by RT–PCR only in the brainstem and spinal cord. No hVAChT mRNA signal was detectable in the forebrain or peripheral organs.

At the cellular level, the expression pattern of hVAChT mRNA was compared to that of mVAChT on coronal sections from frozen brains by ISHH using species-specific riboprobes. The specificity of the hVAChT riboprobe for hVAChT was confirmed by the absence of any ISHH signal in brain sections from non-transgenic mice with strong mVAChT ISHH signals (data not shown). Following the rostrocaudal distribution of cholinergic neurons in the CNS, cholinergic neurons in the medial septal nucleus, the nuclei of the horizontal and vertical limbs of the diagonal band (Fig. 8A), the interneurons in the caudate–putamen (Fig. 8B, C), and the basal nucleus of Meynert (Fig. 8C) all showed robust signals for mVAChT. There was no hVAChT mRNA detectable in any of these cell groups (Fig. 8D–F). In the thalamus, the medial habenular nuclei were strongly labeled with the mVAChT probe (Fig. 8G), but did not show hVAChT signals (Fig. 8H).

The absence of hVAChT mRNA signals in the basal forebrain and diencephalic cholinergic neurons is consistent with the absence of hVAChT immunoreactivity in the projection fields of the main cholinergic circuits arising from these neurons. Neither the Ch4 projection to the neocortex (Fig. 9B) nor the Ch1/Ch2 projections to the hippocampus (Fig. 9D) contained hVAChT-positive fibers or terminals by immunohistochemistry, using a hVAChT-specific antiserum, while endogenous mVAChT was easily detectable in these regions (Fig. 9A, C). In addition, the densely packed neuronal cell bodies of the medial habenular nucleus showed strong immunoreactivity for mVAChT (Fig. 9E), but did not stain for hVAChT (Fig. 9F).

In the brainstem and spinal cord, expression of the hVAChT transgene was detectable in all somatomotor, but not in visceromotor, nuclei (Figs 10, 11). The most rostral cholinergic nucleus of the brain that expressed hVAChT mRNA was the oculomotor nucleus (Fig. 10B), followed by strong signals in the motor nucleus of the trigeminal (Fig. 10D), facial (Fig. 10F) and hypoglossal (Fig. 10H) nerves. In the thoracic spinal cord, hVAChT mRNA was detectable in ventral horn motor neurons, but undetectable in preganglionic sympathetic neurons in the intermediolateral cell column (Fig. 10J). Lack of significant hVAChT mRNA expression was also obvious for the laterodorsal tegmental nucleus of the ascending projection system (Fig. 10D) and for the

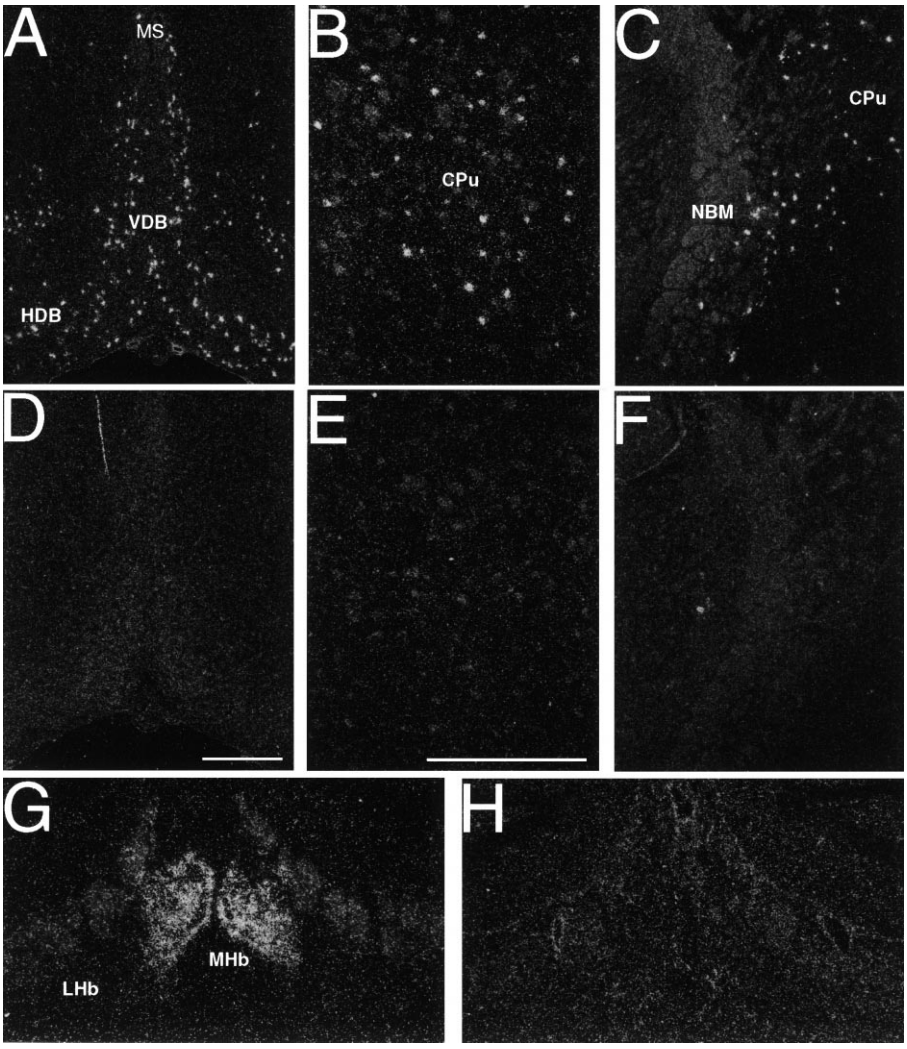


Fig. 8. Lack of expression of hVAChT mRNA in basal forebrain cholinergic neurons of transgenic mice. Dark-field photomicrographs of ISHH with mVAChT (A–C, G) and hVAChT (D–F, H) specific riboprobes on coronal brain sections show that mVAChT mRNA, but not hVAChT mRNA, is expressed in the medial septal nucleus (MS), in the nuclei of the horizontal (HDB) and vertical (VDB) limbs of the diagonal band, in the cholinergic interneurons of the caudate–putamen (CPu), in the nucleus basalis of Meynert (NBM), and in the medial habenular nucleus (MHb). LHb, lateral habenular nucleus. Scale bars = 0.5 mm (D; also applies to A, C, and F), 0.5 mm (E; also applies to B, G and H).

parasympathetic visceroefferent cell group of the motor nucleus of the vagus (Fig. 10H). Signal intensities of hVAChT ISHH varied between individual nuclei. They were strongest in the motor facial nerve, followed by motor trigeminal and ventral horn motor neurons. Signal intensities for hVAChT were lowest in motor nuclei of the oculomotor and hypoglossal nerves.

The restriction of expression of hVAChT to somatomotor neurons was also obvious at the protein level. By using species-specific antisera in immunohistochemical staining, hVAChT immunoreactivity was detectable in cell bodies of the oculomotor nucleus (Fig. 11B), but not in terminals in the interpeduncular nucleus on the same section. Both structures stained intensely using anti-mVAChT antibodies (Fig. 11A). The same hVAChT staining pattern was observable in the more caudally located somatomotor nuclei of the trigeminal (Fig. 11D), abducens (Fig. 11F), facial (Fig. 11H) and hypoglossal (Fig. 11J) nerves. Human VAChT was expressed in many, but not all, cholinergic neurons in these nuclei, consistent with the results obtained by ISHH (see above).

All cholinergic somatomotor neurons in the brainstem project to the periphery, where they form synapses on muscle cells at the motor endplate. To determine if the transgenic hVAChT is transported into motor endplate synapses which contain mVAChT, we analysed sections from the tongues of transgenic animals, the terminal field of the somatomotoric hypoglossal nerve. The tongue is a mostly muscular structure, rich in cholinergic motor endplates. For example, the intensely labeled mVAChT-positive motor endplates appeared as bouton-like structures along muscle fibers in the tongue (Fig. 12A, C, E). The accumulation of the transgenic hVAChT in motor endplates is shown on adjacent sections (Fig. 12B, F), proving that the protein is transported from the site of production in the cell body to the synapse, where synaptic vesicles are abundant.

In addition to receiving cholinergic innervation from the brainstem, the tongue contains cholinergic neurons, which belong to the parasympathetic nervous system. These intrinsic neurons are organized in small ganglia (Fig. 12A), supply local blood vessels (Fig. 12E) and can be identified by mVAChT staining. Transgenic hVAChT was not detectable in the neuronal cell bodies (Fig. 12B) or in the corresponding

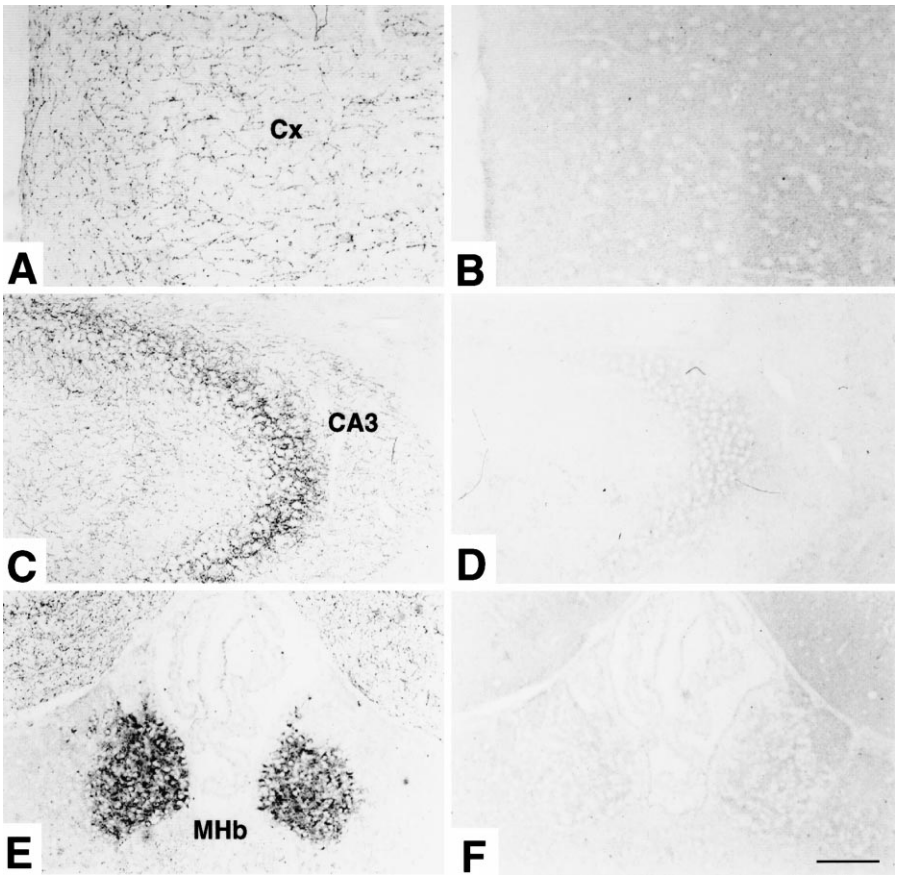


Fig. 9. Human VAChT immunoreactivity is absent from neocortical and thalamic cholinergic cell bodies and terminal fields of transgenic mice. Immunocytochemistry for mVAChT (A, C, E) and hVAChT (B, D, F) on adjacent sections from the cortex (A, B), hippocampus (C, D) and dorsal thalamus (E, F). The extrinsic cholinergic innervation of the cortex (Cx) and the CA3 region of the hippocampus (CA3) can be visualized with anti-mVAChT antibodies, but is negative for hVAChT immunoreactivity. The densely packed cell bodies of the medial habenular nucleus (MHb) stain heavily for mVAChT, whereas no staining is detectable on an adjacent section using an hVAChT-specific antiserum. Scale bar = 100 μm (F; applies to all).

terminals around blood vessels (Fig. 12F), again demonstrating the absence of expression in non-somatomotor neurons.

Cholinergic, autonomic neurons are widely distributed throughout the body, and contribute to the sympathetic, parasympathetic and gut intrinsic nervous systems. The cranial parasympathetic ganglia are 100% cholinergic and represent the largest subdivision with the highest neuron numbers. To rule out the possibility that the lack of hVAChT detection in small intrinsic ganglia is due to a lack of immunocytochemical sensitivity, expression of mVAChT and hVAChT mRNAs was analysed by ISHH in the submandibular ganglion. Mouse mVAChT mRNA (Fig. 13A), but not hVAChT mRNA (Fig. 13C), was expressed in parasympathetic neurons of the peripheral nervous system.

In the gastrointestinal tract, intrinsic cholinergic neurons contribute to the innervation of the gut smooth musculature. Hybridization with the mVAChT-specific probe labeled the neurons of the myenteric (Fig. 13B, arrows) and submucous plexus (Fig. 13B, arrowhead). Both neuronal plexuses were negative for hVAChT mRNA hybridization signals (Fig. 13D).

To show that absence of hVAChT mRNA in all but somatomotor cholinergic neurons is due to lack of expression, rather than failure to see low levels of expression due to lack of sensitivity, we compared hVAChT and mVAChT ISHH in the medial habenular nucleus and the trigeminal motor nucleus across a broad range of exposure times. We chose the medial habenular nucleus and trigeminal motor nucleus because the density of cholinergic neurons in these nuclei is similar and therefore well suited for direct comparison. After 8 h of exposure to X-ray film, mVAChT signals in the trigeminal motor nucleus were twice as strong as mVAChT signals in the medial habenular nucleus and four times stronger than hVAChT signals in the trigeminal motor nucleus (data not shown). The difference in signal intensity between hVAChT and mVAChT in the medial habenular nucleus should therefore be eight-fold. Even after a 72-h exposure time, no signals for hVAChT could be detected in the medial habenular nucleus (data not shown). This is twice the predicted time to visualize hVAChT mRNA in the medial habenular nucleus if expressed at a similar ratio to the trigeminal motor nucleus as that seen for mVAChT, confirming that expression of hVAChT from the hV8.7 transgene is restricted to somatomotor neurons in the mouse.

## DISCUSSION

### *Expression of the vesicular acetylcholine transporter in the mouse nervous system*

Analysis of the expression of VAChT and its mRNA in the mouse CNS confirmed the existence of the fully cholinergic circuits Ch1–Ch8 described based on ChAT immunoreactivity in the primate, and ChAT plus VAChT

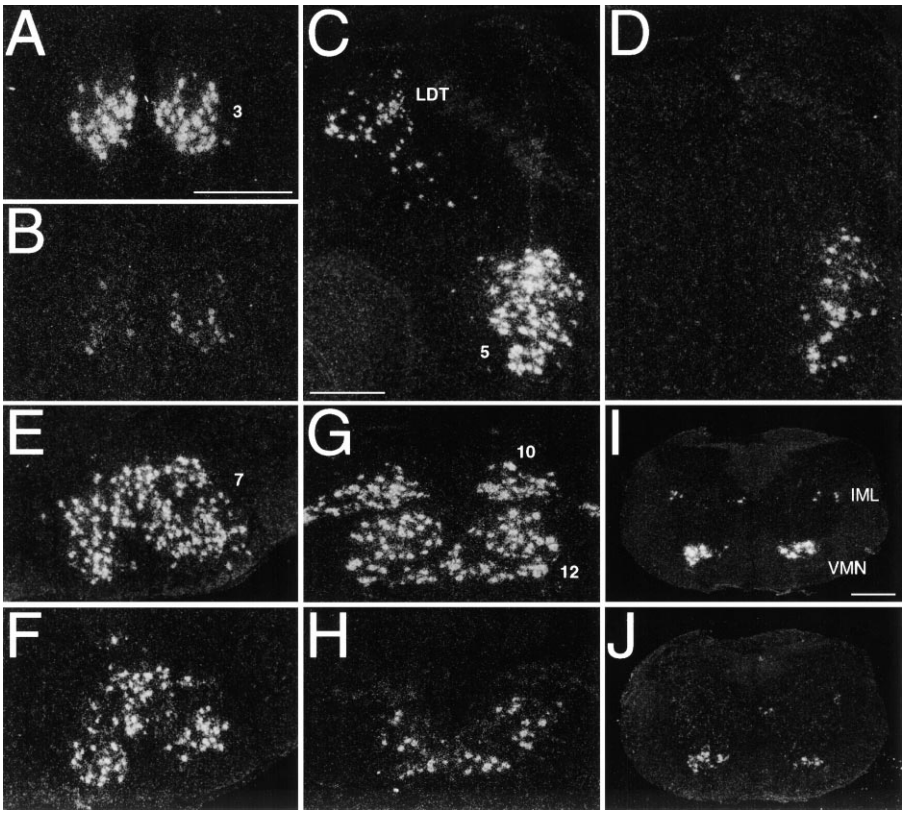


Fig. 10. Human VAChT mRNA is expressed in somatomotor neurons in the brainstem and spinal cord of transgenic mice. Dark-field photomicrographs of ISHH for mVAChT mRNA (A, C, E, G, I) and hVAChT mRNA (B, D, F, H, J) on coronal sections from the brainstem and spinal cord. Mouse VAChT and hVAChT are detected on adjacent sections in cell bodies of the motor nuclei of the oculomotor (3; A, B), trigeminal (5; C, D), facial (7; E, F) and hypoglossal (12; G, H) nerves, and in the motor neurons in the ventral horn of the spinal cord (VMN; I, J). No hVAChT signals are detectable in the projection neurons of the lateral dorsal tegmental nucleus (LDT; D), in the motor nucleus of the vagus (10; H) and in the preganglionic autonomic neurons in the intermediolateral cell column of the spinal cord (IML; J). Note that signal intensities for hVAChT mRNA are highest in motor trigeminal and facial nerves, moderate in the motor hypoglossal nerve and spinal cord, and weakest in the motor oculomotor nerve. Note also that hVAChT mRNA is expressed in many, but not all, cholinergic neurons in each individual nucleus. Scale bars = 0.4 mm (A; also applies to B, G and H), 0.4 mm (C; also applies to D–F), 0.4 mm (I; also applies to G).

immunoreactivity in the rat.[23,24,34,35,46,47] These include: basal forebrain projection systems to the hippocampus (Ch1/Ch2), olfactory cortex (Ch3), and neocortex and amygdala (Ch4); mesopontothalamic projections (Ch5/Ch6); the prominent habenulointerpeduncular projection (Ch7); a cholinergic cell group in the parabigeminal nucleus and cholinergic terminals in superior colliculus (Ch8); and cholinergic interneurons in the striatum and the islands of Calleja. Notably, the abundance and intensity of VAChT innervation in the Ch1–Ch8 projection systems and in basal forebrain and striatal intrinsic neurons is qualitatively similar in mouse compared to rat[35] and primate[36] (Weihe *et al*., unpublished observations).

VAChT immunoreactivity and mRNA were undetectable in neuronal soma in the hippocampus and frontal, temporal, parietal and occipital cortex of the mouse. Despite reports of ChAT immunoreactivity in rat hippocampal neurons,[11] neither VAChT immunoreactivity nor mRNA are localized to hippocampal neurons in the rat[35] or mouse (this report). On the other hand, both VAChT and ChAT and their mRNAs have been localized to cerebrocortical neurons in the rat and primate, with a widespread but sparse distribution, suggesting a functional role for cholinergic intrinsic neurons in the cortex of these species.[35,36]

Cholinergic circuitry in the mouse brain is otherwise strikingly similar to that in other mammals, reinforcing the use of both mouse and rat models of cholinergic dysfunction and neurodegeneration, and their impact on cognitive function.[3,10,49] Likewise, the heavy innervation of the median eminence of the hypothalamus by VAChT-positive terminals in the mouse, as in the rat and primate, confirms the relevance of studies in the mouse of cholinergic involvement in hypothalamopituitary function to human neuroendocrine regulation by acetylcholine. The cholinergic innervation of the median eminence in the mouse, as in the rat, likely arises from projections of VAChT/ChAT-positive cell bodies in the arcuate nucleus and, more diffusely, in the ventromedial nucleus.[35,42]

### *Comparison of mouse and human cholinergic gene locus upstream regulatory sequences*

The mouse CGL sequence shows a high degree of homology with both the rat and human cholinergic gene loci in regions implicated previously in cholinergic cell-specific transcription,[22] responsiveness to NGF[5,16] and silencing of the CGL in non-neuronal cells.[13,22] The high level of mammalian sequence identity for these putative *cis*-acting elements within the CGL suggests their importance in transcriptional regulation of the CGL *in vivo*.

A cholinergic enhancer domain has been identified in the distal region of the CGL using a fragment of the rat CGL fused to a heterologous promotor with reporter gene activity initiating from the putative R-exon transcriptional start site.[22] An NGF-responsive element has been identified proximal to the R-exon in a CGL–chloramphenical reporter fusion gene,

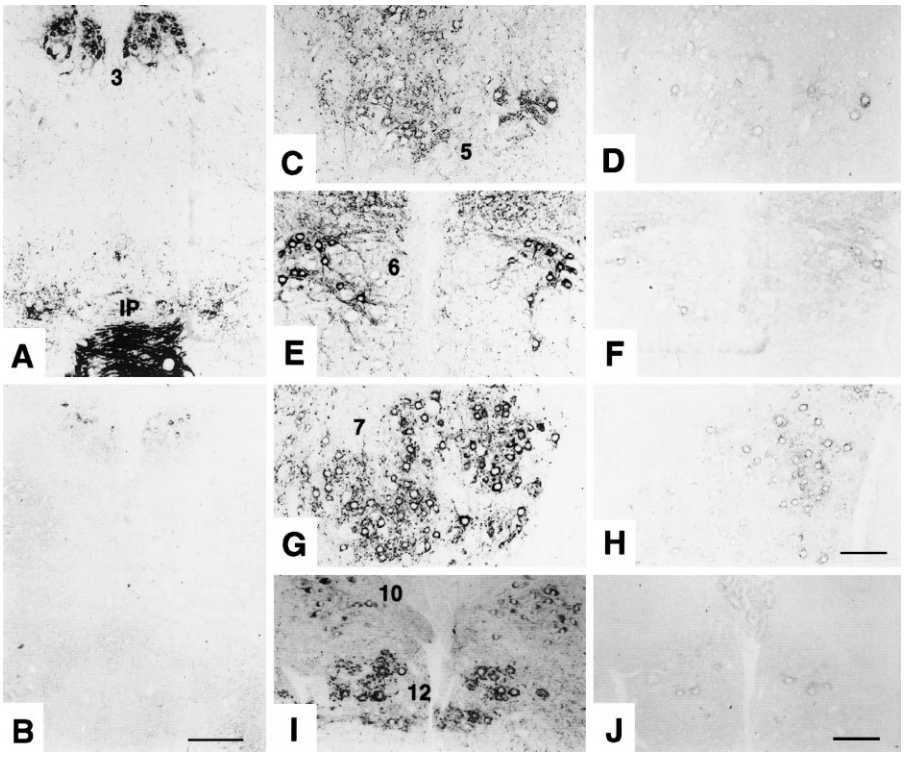


Fig. 11. Human VAChT immunoreactivity is present in the cell bodies of somatomotor neurons, but absent from visceromotor neurons and projection neuron terminal fields. (A, B) Immunocytochemistry for mVAChT (A) and hVAChT (B) on adjacent sections through the brainstem of transgenic mice. Mouse VAChT immunoreactivity is detectable in the cell bodies of the oculomotor nucleus (3) and in terminals in the interpeduncular nucleus (IP). Human VAChT-immunoreactive cell bodies can be detected in the oculomotor nucleus, but terminal staining is completely absent in the interpeduncular nucleus. (C–J) Mouse VAChT immunoreactivity was used to identify additional cholinergic somatomotor and visceromotor nuclei in the brainstem, shown here for the trigeminal (5; C), abducens (6; E), facial (7; G), vagal (10; I) and hypoglossal (12; I) nuclei. On adjacent sections, hVAChT immunoreactivity is present in all somatomotor nuclei (D, F, H, J), but absent from the vagal visceromotor nucleus (J). Scale bars = 200 μm (B; also applies to A), 100 μm (H, J; also applies to C–G and I).

also initiating transcription from the "R" promoter, transiently expressed in fetal rat septohippocampal cultured neurons.[5] It is difficult to evaluate whether or not these two *cis*-regulatory domains regulate both VAChT and ChAT transcription *in vivo*, since the transcriptional start site at the R-exon, common to both VAChT and ChAT, appears to be only a minor transcriptional start site *in vivo*.[13] However, in a recent study by Oosawa *et al.*,[28] both VAChT and ChAT mRNAs were elevated in response to NGF treatment of primary cultured rat embryonic septal cells, indicating coordinated control of VAChT and ChAT promoters by an NGF-response element in the CGL.

An NRSE contained in the upstream region of the CGL has been shown to be important for neuronally restricted expression, in cultured rat and human cell lines.[13,22] This is the only element within the mouse CGL that matches the consensus sequence developed by Schoenherr and Anderson[38] for an NRSE. Thus, the reported restriction of a mouse CGL transgene lacking the NRSE to cholinergic neurons *in vivo* suggests that other elements conferring non-neuronal silencing exist elsewhere in the CGL.[26]

### *Expression of the vesicular acetylcholine transporter from the human cholinergic gene locus in the mouse*

Attempts to identify regulatory regions in the CGL that are important for the expression of VAChT and ChAT have mainly focused on testing the ability of fragments from the CGL to drive reporter gene expression in cell lines or primary cholinergic cells in culture.[13,22] These experiments have provided significant information about the type and number of potential *cis*-regulatory elements contributing to cholinergic expression that can now be addressed *in vivo*. Two studies have addressed the regulation of the ChAT gene in transgenic mice. Lönnerberg *et al.*[21] demonstrated reporter gene expression in the ventral spinal cord and brain when 2 kb of the rat CGL, comprising the NRSE and sequences flanking it, were attached to a heterologous promoter driving the chloramphenicol acetyltransferase gene. Naciff and Dedman[26] introduced 6.1 kb of the mouse CGL from 600 bp upstream of the VAChT initiation codon to the first ChAT coding exon, fused to β-galactosidase, into transgenic mice: expression of β-galactosidase appropriate to cholinergic neurons, albeit at low levels, was observed in the CNS. Removal of sequences containing the VAChT open reading frame resulted in increased expression of β-galactosidase within non-cholinergic neurons in the CNS, suggesting that the VAChT gene itself contains sequences required for cholinergic-specific ChAT gene expression.

From these studies, it became clear that the ChAT gene could be controlled by separate elements both upstream and downstream of the start of transcription of the VAChT gene. We wished to focus on the expression of VAChT itself from the CGL, to begin to identify the *cis*-regulatory elements of the CGL that control VAChT and ChAT transcription both separately and coordinately. To examine VAChT gene regulation without replacing potential *cis*-regulatory elements in the VAChT open reading frame with a reporter gene, we introduced the well-conserved human CGL, including hVAChT itself, into the mouse germline, and monitored

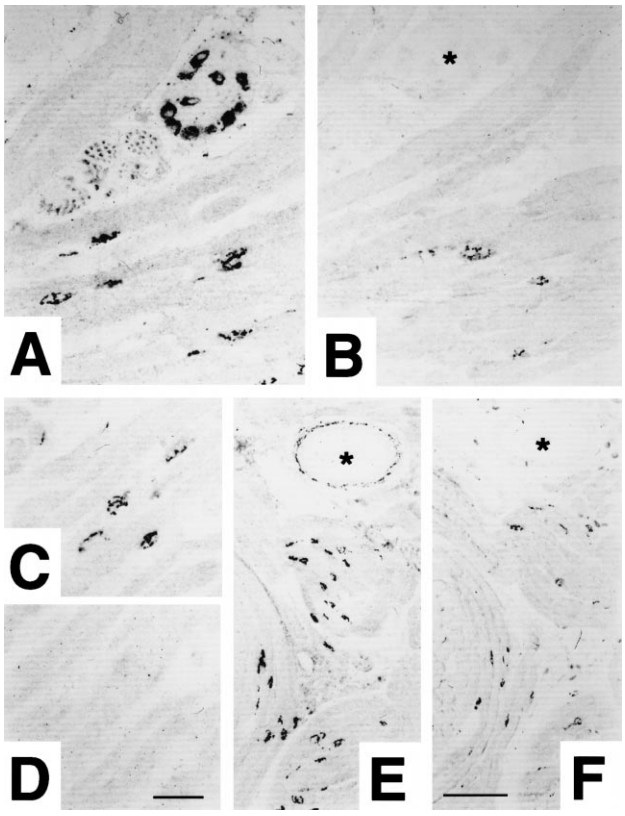


Fig. 12. Human VAChT immunoreactivity is present in motor endplates of the tongue, but not in autonomic neurons and associated terminal fields. Mouse VAChT immunoreactivity was used to identify cholinergic motor endplates along muscle fibres in the tongue of transgenic (A) and non-transgenic (C) mice. In transgenic animals, these motor endplates also stain for hVAChT (B), whereas staining is completely absent from motor endplates of non-transgenic animals (D), confirming the specificity of the anti-hVAChT antiserum. The neuronal profiles of an intrinsic parasympathetic ganglion stain positive for mVAChT (A), but are negative for hVAChT (B, asterisk). The absence of hVAChT in autonomic neurons is reflected by the absence of corresponding fiber staining in varicose fibers supplying local blood vessels (F, asterisk). Note equally strong mVAChT terminal staining around blood vessels (E, asterisk) and along the musculature. Scale bars = 25 μm (D; also applies to A–C), 100 μm (F; also applies to E).

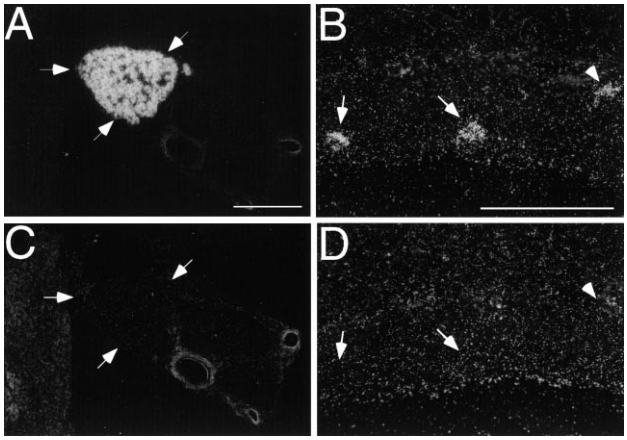


Fig. 13. Lack of expression of hVAChT mRNA in peripheral parasympathetic ganglia. Dark-field photomicrographs of ISHH experiments illustrate that mVAChT mRNA (A, B), but not hVAChT mRNA (C, D), is expressed in a parasympathetic ganglion in the submandibular gland (left panels) and in gut intrinsic cholinergic neurons (right panels). The arrows in B and D point toward ganglia in the myenteric plexus, the arrowhead toward a ganglion in the submucous plexus. Scale bars = 250 μm (A; also applies to C, B; also applies to D).

expression of transgenic VAChT using species-specific hVAChT PCR primer pairs, riboprobes and antibodies.

The region of the CGL we chose extended 5′ through all known putative regulatory elements of the VAChT and ChAT genes up to the matrix attachment site identified previously in the human gene,[44] and 3′ to the M-exon, considered to be the most 3′ major transcriptional start point for the ChAT gene.[17,25] We found that (i) this construct was not ectopically expressed in the mouse and (ii) VAChT expression was limited to somatomotor neurons of the CNS.

Lack of ectopic VAChT transcription of the human CGL transgene is itself of significant interest, since both the VAChT and ChAT promoters drive robust transcription when removed from the CGL and placed in front of reporter genes, both in neurons and in non-neuronal cell lines in culture.[6,14,20] This finding is consistent with the observation that the entire 5′ flank of this transgene, fused to a reporter gene at the hVAChT promoter, is expressed at high levels in both cholinergic and non-cholinergic cell lines upon removal of NRSE-containing sequences.[13] Thus, strong ChAT and VAChT promoters, shown to be non-cell specific in isolation from the CGL, are adequately silenced by regulatory sequences contained in the transgene.

Restriction of expression of the hV8.7 transgene to somatomotor neurons was an unexpected finding. It implies that regulation of the CGL in this subdivision of the cholinergic nervous system is unique and separable from cholinergic regulation elsewhere, and that additional upstream or downstream sequences of the CGL are required for full cholinergic expression *in vivo*. A bHLH protein, MNR2, is expressed uniquely in somatomotor neurons (and not in visceromotor or other cholinergic neurons) in the chicken, and its ectopic expression induces the cholinergic phenotype in the developing chicken spinal cord.[43] MNR2 may directly or indirectly regulate CGL transcription in visceromotor neurons *in vivo*, via a *cis*-reglatory element present in the hV8.7 transgene.

Where might additional sequences controlling non-somatomotor cholinergic expression be located within the CGL? The 5′ flank of the hV8.7 transgene extends to the proposed matrix attachment site reported by Tanaka *et al.*[44] It is therefore unlikely that additional 5′ sequences are required. The hV8.7 transgene lacks 2.5 kb of 3′ sequence between the "M" non-coding and the first coding exon of ChAT. Quirin-Stricker *et al.*[29] have recently identified a sequence element in this region of the human CGL which functions as a thyroid hormone response element and is conserved in the mouse gene (see Accession no. AF019045 for the mouse sequence). In view of the restricted expression of hV8.7, and the low-level but pan-cholinergic expression of the mouse construct of Naciff and Dedman,[26] it is likely that sequences absent from the latter construct and present in hV8.7 are responsible for both enhanced cholinergic and silenced non-neuronal transcription of the CGL, while 3′ sequences present in this construct but lacking from hV8.7 are responsible for controlling CGL trancription in non-somatomotor cholinergic neurons. Experiments to test these hypotheses are in progress.

*Acknowledgements*—We wish to thank Dr Huiyan Lu of the National Center for Research Resources for assistance with the construction of the three lines of hVAChT transgenic mice described here, and Dr Ed Ginns, NIMH Transgene Facility, for consultation on development of

additional hVAChT transgenic mouse lines. The excellent technical help of Rita Vertesi, Florencia Nochetto, Petra Lattermann, Elke Rodenberg, Petra Sack and Marion Hainmüller is gratefully acknowledged. We thank Heidemarie Schneider and Ricardo Dreyfuss for excellent photodocumentation. This work was supported in part by grants from the German Research Foundation (SFB 297), the Volkswagen-Stiftung and the Kempkes Stiftung Marburg.

## REFERENCES

1. Alfonso A., Grundahl K., McManus J. R., Asbury J. M. and Rand J. B. (1994) Alternative splicing leads to two cholinergic proteins in *C. elegans*. *J. molec. Biol.* **241,** 627–630.
2. Angerer L. M., Stoler M. H. and Angerer R. C. (1987) *In situ* hybridization with RNA probes: an annotated recipe. In In Situ *Hybridization: Applications to Neurobiology*, (eds Valentino, K. L., Eberwine J. H. and Barchas J. D.), p. 42. Oxford University Press, New York.
3. Baxter M. G., Frick K. M., Price D. L., Breckler S. J., Markowska A. L. and Gorman L. K. (1999) Presynaptic markers of cholinergic function in the rat brain: relationship with age and cognitive status. *Neuroscience* **89,** 771–780.
4. Bejanin S., Cervini R., Mallet J. and Berrard S. (1994) A unique gene organization for two cholinergic markers, choline acetyltransferase and a putative vesicular transporter of acetylcholine. *J. biol. Chem.* **269,** 21944–21947.
5. Bejanin S., Habert E., Berrard S., Edwards J.-B. D. M., Loeffler J.-P. and Mallet J. (1992) Promoter elements of the rat choline acetyltransferase gene allowing nerve growth factor inducibility in transfected primary cultured cells. *J. Neurochem.* **58,** 1580–1583.
6. Cervini R., Houhou L., Pradat P.-F., Bejanin S., Mallet J. and Berrard S. (1995) Specific vesicular acetylcholine transporter promoters lie within the first intron of the rat choline acetyltransferase gene. *J. biol. Chem.* **270,** 24654–24657.
7. Chong J. A., Tapia-Ramirez J., Kim S., Toledo-Arai J. J., Zheng Y., Boutros M. C., Altshuller Y. M., Frohman M. A., Kraner S. D. and Mandel G. (1995) REST: a mammalian silencer protein that restricts sodium channel gene expression to neurons. *Cell* **80,** 949–957.
8. Eiden L. E. (1998) The cholinergic gene locus. *J. Neurochem.* **70,** 2227–2240.
9. Erickson J. D., Varoqui H., Schäfer M., Diebler M.-F., Weihe E., Modi W., Rand J., Eiden L. E., Bonner T. I. and Usdin T. (1994) Functional characterization of the mammalian vesicular acetylcholine transporter and its expression from a 'cholinergic' gene locus. *J. biol. Chem.* **269,** 21,929–21,932.
10. Fischer W., Wictorin K., Bjorklund A., Williams L. R., Varon S. and Gage F. H. (1987) Amelioration of cholinergic neuron atrophy and spatial memory impairment in aged rats by nerve growth factor. *Nature* **329,** 65–68.
11. Frotscher M. and Leranth C. (1985) Cholinergic innervation of the rat hippocampus as revealed by choline acetyltransferase immunocytochemistry, a combined light and electron microscopic study. *J. comp. Neurol.* **239,** 237–246.
12. Gilmor M. L., Nash N. R., Roghani A., Edwards R. H., Yi H., Hersch S. M. and Levey A. I. (1996) Expression of the putative vesicular acetylcholine transporter in rat brain and localization in cholinergic synaptic vesicles. *J. Neurosci.* **16,** 2179–2190.
13. Hahm S. H., Chen L., Patel C., Erickson J., Bonner T. I., Weihe E., Schäfer M. K.-H. and Eiden L. E. (1997) Upstream sequencing and functional characterization of the human cholinergic gene locus. *J. molec. Neurosci.* **9,** 223–236.
14. Hersh L. B., Inoue H. and Li Y.-P. (1996) Transcriptional regulation of the human choline acetyltransferase gene. *Prog. Brain Res.* **109,** 47–54.
15. Hersh L. B., Kong C. F., Sampson C., Mues G., Li Y.-P., Fisher A., Hilt D. and Baetge E. E. (1993) Comparison of the promoter region of the human and porcine choline acetyltransferase genes: localization of an important enhancer region. *J. Neurochem.* **61,** 306–314.
16. Ibanez C. F. and Persson H. (1991) Localization of sequences determining cell type specificity and NGF responsiveness in the promoter region of the rat choline acetyltransferase gene. *Eur. J. Neurosci.* **3,** 1309–1315.
17. Kengaku M., Misawa H. and Deguchi T. (1993) Multiple mRNA species of choline acetyltransferase from rat spinal cord. *Molec. Brain Res.* **18,** 71–76.
18. Kitamoto T., Wang W. and Salvaterra P. M. (1998) Structure and organization of the *Drosophila* cholinergic locus. *J. biol. Chem.* **273,** 2706–2713.
19. Kitt C. A., Hohmann C., Coyle J. T. and Price D. L. (1994) Cholinergic innervation of mouse forebrain structures. *J. comp. Neurol.* **341,** 117–129.
20. Li Y.-P., Baskin F., Davis R., Wu D. and Hersh L. B. (1995) A cell type-specific silencer in the human choline acetyltransferase gene requiring two distinct and interactive E boxes. *Molec. Brain Res.* **30,** 106–114.
21. Lönnerberg P., Lendahl U., Funakoshi H., Arhlund-Richter L., Persson H. and Ibanez C. F. (1995) Regulatory region in choline acetyltransferase gene directs developmental and tissue-specific expression in transgenic mice. *Proc. natn. Acad. Sci. U.S.A.* **92,** 4046–4050.
22. Lönnerberg P., Schoenherr C. J., Anderson D. J. and Ibanez C. F. (1996) Cell type-specific regulation of choline acetyltransferase gene expression. Role of the neuron-restrictive silencer element and cholinergic-specific enhancer sequences. *J. biol. Chem.* **271,** 33358–33365.
23. Mesulam M.-M. (1990) Human brain cholinergic pathways. In *Progress in Brain Research* (eds Aquilonius S.-M. and Gillberg P.-G.), Vol. 84, pp. 231–241. Elsevier Science, Amsterdam.
24. Mesulam M.-M., Mufson E. J., Wainer B. H. and Levey A. I. (1983) Central cholinergic pathways in the rat: an overview based on an alternative nomenclature (Ch1–Ch6). *Neuroscience* **10,** 1185–1201.
25. Misawa H., Ishii K. and Deguchi T. (1992) Gene expression of mouse choline acetyltransferase: alternative splicing and identification of a highly active promoter region. *J. biol. Chem.* **267,** 20392–20399.
26. Naciff J. and Dedman J. (1999) Identification and transgenic analysis of a murine promoter that targets cholinergic neuron expression. *J. Neurochem.* **72,** 17–28.
27. Naciff J. M., Misawa H. and Dedman J. R. (1997) Molecular characterization of the mouse vesicular acetylcholine transporter gene. *NeuroReport* **8,** 3467–3473.
28. Oosawa H., Fujii T. and Kawashima K. (1999) Nerve growth factor increases the synthesis and release of acetylcholine and the expression of vesicular acetylcholine transporter in primary cultured rat embryonic septal cells. *J. Neurosci. Res.* **57,** 381–387.
29. Quirin-Stricker C., Nappy V., Simoni P., Toussaint J. L. and Schmitt M. (1994) Trans-activation by throid hormone receptors of the 5′ flanking region of the human ChAT gene. *Molec. Brain Res.* **23,** 253–265.
30. Roghani A., Shirzadi A., Butcher L. L. and Edwards R. H. (1998) Distribution of the vesicular transporter for acetylcholine in the rat central nervous system. *Neuroscience* **82,** 1195–1212.
31. Röhrenbeck A. M., Bette M., Hooper D. C., Nyberg F., Eiden L. E., Dietzschold B. and Weihe E. (1999) Upregulation of COX-2 and CGRP expression in resident cells of the Borna disease virus-infected brain is dependent upon inflammation. *Neurobiol. Dis.* **6,** 15–34.
32. Sambrook J., Fritsch E. F. and Maniatis T. (1989) *Molecular Cloning: A Laboratory Manual*, 2nd edn. Cold Spring Harbor Laboratory, Cold Spring Harbor, NY.
33. Sanger F., Nicklen S. and Coulson A. R. (1977) DNA sequencing with chain terminating inhibitors. *Proc. natn. Acad. Sci. U.S.A.* **74,** 5463–5467.
34. Schäfer M. K.-H., Eiden L. E. and Weihe E. (1998) Cholinergic neurons and terminal fields revealed by immunohistochemistry for the vesicular acetylcholine transporter—II. The peripheral nervous system. *Neuroscience* **84,** 361–376.
35. Schäfer M. K.-H., Eiden L. E. and Weihe E. (1998) Cholinergic neurons and terminal fields revealed by immunohistochemistry for the vesicular acetylcholine transporter—I. Central nervous system. *Neuroscience* **84,** 331–359.
36. Schäfer M. K.-H., Weihe E., Erickson J. D. and Eiden L. E. (1995) Human and monkey cholinergic neurons visualized in paraffin-embedded tissues by immunoreactivity for VAChT, the vesicular acetylcholine transporter. *J. molec. Neurosci.* **6,** 225–235.
37. Schäfer M. K.-H., Weihe E., Varoqui H., Eiden L. E. and Erickson J. D. (1994) Distribution of the vesicular acetylcholine transporter (VAChT) in the central and peripheral nervous systems of the rat. *J. molec. Neurosci.* **5,** 1–18.

38. Schoenherr C. J. and Anderson D. J. (1995) The neuron-restrictive silencer factor (NRSF): a coordinate repressor of multiple neuron-specific genes. *Science* **267,** 1360–1363.
39. Schütz B., Schäfer M. K.-H., Eiden L. E. and Weihe E. (1998) Vesicular amine transporter expression and isoform selection in developing brain, peripheral nervous system and gut. *Devl Brain Res.* **106,** 181–204.
40. Semba K. and Fibiger H. C. (1989) Organization of central cholinergic systems. In *Progress in Brain Research* (eds Nordberg A., Fuxe K., Holmstedt B. and Sundwall A.), Vol. 79, pp. 37–63. Elsevier Science, Amsterdam.
41. Steriade M. and Buzsaki G. (1990) Parallel activation of thalamic and cortical neurons by brainstem and basal forebrain cholinergic systems. In *Brain Cholinergic Systems* (eds Steriade M. and Biesold D.), pp. 3–62. Oxford University Press, Oxford.
42. Tago H., McCeer P. L., Bruce G. and Hersh L. B. (1987) Distribution of choline acetyltransferase-containing neurons of the hypothalamus. *Brain Res.* **415,** 49–62.
43. Tanabe Y., William C. and Jessell T. M. (1998) Specification of motor neuron identity by the MNR2 homeodomain protein. *Cell* **95,** 67–80.
44. Tanaka H., Zhao Y., Wu D. and Hersh L. B. (1998) The use of DNase I hypersensitivity site mapping to identify regulatory regions of the human cholinergic gene locus. *J. Neurochem.* **70,** 1799–1808.
45. Usdin T., Eiden L. E., Bonner T. I. and Erickson J. D. (1995) Molecular biology of vesicular acetylcholine transporters (VAChTs). *Trends Neurosci.* **18,** 218–224.
46. Wainer B. H., Levey A. I., Mufson E. J. and Mesulam M. M. (1984) Cholinergic systems in mammalian brain identified with antibodies against choline acetyltransferase. *Neurochem. Int.* **2,** 163–182.
47. Wainer B. H. and Mesulam M.-M. (1990) Ascending cholinergic pathways in the rat brain. In *Brain Cholinergic Systems* (eds Steriade M. and Biesold D.), pp. 65–119. Oxford University Press, Oxford.
48. Weihe E., Tao-Cheng J.-H., Schäfer M. K.-H., Erickson J. D. and Eiden L. E. (1996) Visualization of the vesicular acetylcholine transporter in cholinergic nerve terminals and its targeting to a specific population of small synaptic vesicles. *Proc. natn. Acad. Sci. U.S.A.* **93,** 3547–3552.
49. Winkler J., Thal L. J. and Gage F. H. (1998) Cholinergic strategies for Alzheimer's disease. *J. molec. Med.* **76,** 555–567.

(*Accepted* 8 *December* 1999)